JOURNAL OF MATERIALS SCIENCE 30 (1995) 4906–4911

Deformation mechanism map for creep in $YBa_2Cu_3O_{7-x}$

J. YUN, M.P. HARMER, Y.T. CHOU
Department of Materials Science and Engineering and Materials Research Center, Lehigh University, Bethlehem, PA 18015, USA

A deformation mechanism map with grain size and stress as variables was constructed for creep in $YBa_2Cu_3O_{7-x}$ at 850 and 950 °C. Theoretical models of Nabarro–Herring, Coble, and power-law creep were used for the construction. The values of various physical constants for creep of $YBa_2Cu_3O_{7-x}$ were taken from the literature, or estimated with appropriate assumptions. The constructed map showed that the Nabarro–Herring creep would dominate at high temperatures in the practical range of grain size and stress, and that the power-law creep would occur at large stress (> 1 GPa) and grain size. A review of previous creep studies showed that the map is in close agreement with the experimental results. Discrepancies in the values of stress exponent and activation energy for creep of $YBa_2Cu_3O_{7-x}$ given in the literature are explained by the use of the constructed map.

1. Introduction

Although a number of deformation processes with different mechanisms may simultaneously occur during the plastic deformation of metals or ceramics, more frequently a single mechanism would favourably dominate the deformation under a given set of conditions. The predominating deformation mechanism is determined by four main variables; the strain rate, the applied stress, the temperature, and the grain size of a test sample. Because the deformation mechanism is sensitive to these variables, a comprehensive understanding is very difficult. However, the deformation mechanism map, as proposed by Ashby [1], may lead to a better understanding. Such a map visually characterizes the predominant deformation mechanisms located in a field of two coordinates, temperature and applied stress. Another type of deformation mechanism map, later developed by Mohamed and Langdon [2], uses the grain size and stress as the coordinates. The advantage of a deformation map is its use as a pedagogic, predictive, and extrapolative tool for identification of the deformation mechanisms which take place in the deformation process [3].

The application of the deformation map to the study of creep in $YBa_2Cu_3O_{7-x}$ is advantageous, especially when discrepancies are found in the experimental data. The previous studies of deformation mechanisms in $YBa_2Cu_3O_{7-x}$ [4–8] indeed contain such discrepancies in the stress exponent, n, the activation energy, Q, and, consequently, the deformation mechanism. These will be reviewed.

Table I shows a list of previous studies for creep in $YBa_2Cu_3O_{7-x}$. Stumberg *et al.* [4] studied the high-temperature deformation behaviour at temperatures between 870 and 980 °C. They obtained a stress exponent of 1.0 at 930 °C, and an activation energy of 800 kJ mol^{-1}, and concluded that the creep rate was controlled by the lattice diffusion of cations through the interstitial sites. Goretta *et al.* [5] later carried out a more detailed study using high phase-purity $YBa_2Cu_3O_{7-x}$, and obtained the same stress exponent of 1 and a higher activation energy of 970 ± 130 kJ mol^{-1}. The grain-size exponent determined was 2.8 ± 0.6. It was suggested that the deformation mechanism was the diffusional creep controlled by the diffusion of yttrium or barium atoms. Reyes-Morel *et al.* [6] also obtained a similar value for the stress exponent, 1.25, and concluded that the controlling mechanism was the cation lattice diffusion. They observed two different activation energies, 1220 kJ mol^{-1} in the temperature range 860–890 °C, and 565 kJ mol^{-1} in 800–860 °C.

Two research groups have observed a stress exponent higher than 2. Bussod *et al.* [7] tested $YBa_2Cu_3O_{7-x}$ samples in compression with a confining pressure of 1 GPa, which developed a triaxial stress state inside the samples. They found that the stress exponent was 2.5, much higher than 1 in the case of the uniaxial compression. The activation energy was 201 kJ mol^{-1}, which was much lower than the values reported by the other workers. Kodama and Wakai [8] tested $YBa_2Cu_3O_{7-x}$ samples in uniaxial compression and observed a yield-drop due to crack formation in the early stages of the test. Nonetheless, they determined n and Q by taking the maximum stress as the flow stress and plotting the data against the strain rate or $1/T$. The measured values of n and Q were 2–2.5, and 1080 kJ mol^{-1}, respectively.

As described above, there is an inconsistency in the reported data for n and Q, which might have stemmed from the differences in experimental conditions, such as grain size, temperature, and applied stress. If so, the

0022–2461

TABLE I Data of the previous studies on high-temperature deformation of $YBa_2Cu_3O_{7-x}$

Temperature Range (°C)	n	p	$2Q$ (kJ mol^{-1})	Grain size (μm)	Remark	Reference
870–980	1.0	–	800 ± 100	20–100[a]	–	[4]
850–980	1.0	2.8 ± 0.6	970 ± 130	7–76	–	[5]
860–890	–	–	1220	–	–	[6]
800–860	1.25	–	565	–	–	[6]
750–950	2.5	–	201	10–50*	HC[b]	[7]
850–960	2.5	–	1080	–	YD[c]	[8]

[a] Estimated from the published micrograph or from the sintering conditions.
[b] HC, hydrostatic compression.
[c] YD, yield drop, or decrease in flow stress after a maximum.

variation in these variables should be taken into account when the deformation behaviour under different conditions are compared. For such a comparative study, the deformation mechanism map was found to be useful. However, no previous attempt has been made to construct such a map except for the work of Borofka *et al.* [9] on the hot isostatic pressing (HIP) map for $YBa_2Cu_3O_{7-x}$.

The purposes of the present study were to construct a deformation mechanism map, to critically review the previous results with the aid of the constructed map, and to achieve a comprehensive understanding of the creep behaviour in $YBa_2Cu_3O_{7-x}$.

2. Construction of deformation map for creep in $YBa_2Cu_3O_{7-x}$

In this section, a Langdon-type deformation map for creep of $YBa_2Cu_3O_{7-x}$ is constructed. The map visually shows the controlling mechanisms at a given temperature, grain size and stress. Initially, three processes, which are most prevalent in ceramics, are considered: Nabarro–Herring creep (NHC), Coble creep (CC), and power-law creep (PLC). The corresponding flow equations are given by

$$\dot{\varepsilon} = \frac{B\Omega D_l}{kT}\frac{\sigma}{d^2} \quad \text{(NHC)} \tag{1}$$

$$\dot{\varepsilon} = \frac{150\Omega\delta D_{gb}}{\pi kT}\frac{\sigma}{d^3} \quad \text{(CC)} \tag{2}$$

$$\dot{\varepsilon} = \frac{AD_lG\boldsymbol{b}}{kT}\left(\frac{\sigma}{G}\right)^n \quad \text{(PLC)} \tag{3}$$

where $\dot{\varepsilon}$ is the strain rate, Ω the atomic volume, δ the grain boundary width, G the shear modulus, D_l the lattice diffusivity, D_{gb} the grain boundary diffusivity, σ the flow stress, d the grain size, T the absolute temperature, k Boltzmann's constant, n the stress exponent with a value of 3–5, $\boldsymbol{b}$ the Burgers vector and A and B are constants. The diffusivity term in Equation 3 is originally either for lattice or pipe diffusion, depending on the temperature range. Because the value of homologous temperature is high, ~0.8 at the test temperatures, the pipe diffusion is not likely to occur, and the lattice diffusivity, D_l, is used for the diffusivity in the equation.

On the deformation map, a particular mechanism dominates ($\dot{\varepsilon}_1 \gg \dot{\varepsilon}_2$) inside a domain surrounded by the boundary. On the boundary, two mechanisms corresponding to two contacting domains would have comparable creep rates ($\dot{\varepsilon}_1 = \dot{\varepsilon}_2$), and equally contribute to the total deformation. By equating the strain rates of the two processes and assuming $\delta = 2b$, the equations for the boundaries are obtained

$$\frac{d}{\boldsymbol{b}} = \frac{300D_{gb}}{B\pi D_l} \quad \text{(NHC – CC)} \tag{4}$$

$$\frac{d}{\boldsymbol{b}} = \left(\frac{300\Omega}{A\pi\boldsymbol{b}^3}\frac{D_{gb}}{D_l}\right)^{\frac{1}{3}}\left(\frac{\sigma}{G}\right)^{-(n-1)/3} \quad \text{(PLC – CC)} \tag{5}$$

At the triple point where the NHC, CC and PLC meet, the strain rates of all three processes are equal. By equating Equations 1–3, the normalized stress at the triple point is obtained

$$\frac{\sigma}{G} = \left(\frac{B^3\pi^2\Omega}{A300^2\boldsymbol{b}^3}\frac{D_l^2}{D_{gb}^2}\right)^{1/(n-1)} \tag{6}$$

3. Physical constants for construction of the map

The values for the various physical constants in Equations 4–6 are required to construct a deformation mechanism map. They are determined either from literature data or by the estimation with appropriate assumptions. The details are described below.

3.1. Atomic volume

By definition, atomic volume is the volume transported when a single atom moves. In the mono-component alloy such as a pure metal, it is the volume occupied by an atom in the lattice. In a multi-component system such as a ceramic, a group of atoms move together to maintain the equilibrium, and the atomic volume is the volume of the unit cell divided by the number of atoms of the controlling species in the unit cell. In $YBa_2Cu_3O_{7-x}$, yttrium is the slowest species [10]. Because there is only one yttrium atom in the unit cell, all atoms in the unit cell have to move when the yttrium atom moves. The atomic volume, Ω, is

then the same as the volume of the unit cell

$$\Omega = 3.87 \times 3.87 \times 11.71 \times 10^{-30}\ \mathrm{m}^3$$
$$= 1.754 \times 10^{-28}\ \mathrm{m}^3 \quad (7)$$

3.2. Burgers vector and grain-boundary width

In $YBa_2Cu_3O_{7-x}$, dislocations are primarily of [1 0 0] or [0 1 0] type on the (1 0 0), (0 1 0), and (0 0 1) slip planes [11]. The Burgers vectors for these dislocations are the same, because the crystal structure is tetragonal at high temperatures and the lattice parameters along a and b axes are the same, giving the value of the Burgers vector, $\boldsymbol{b} = 3.87 \times 10^{-10}$ m.

The data for the grain-boundary width in $YBa_2Cu_3O_{7-x}$ are not available. It is usually assumed to be twice as much as that of the Burgers vector or $\delta = 2\boldsymbol{b} = 7.74 \times 10^{-10}$ m [12].

3.3. The shear modulus

The elastic properties of $YBa_2Cu_3O_{7-x}$ have been studied by a group of investigators. Some studies were carried out on the temperature effect on the elastic modulus. However, they were mainly concentrated in the temperature range near the transition temperature ($T_c = -180°$ C). An extrapolation to higher temperatures was not possible because most of the data were scattered, non-linear and anomalous. Jiang *et al.* [13] showed that $\mathrm{d}(f^2)/\mathrm{d}T$ is clearly monotonic in the temperature range 100–300 K, where f is the resonant frequency. However, the uncertainty of the proportionality constant ($E = Cf^2$) in their report made the estimation of $\mathrm{d}E/\mathrm{d}T$ impossible.

Because the elastic property depends on crystal structure, the elastic modulus–temperature dependence in materials with the same crystal structure may be similar to each other. The $\mathrm{d}E/\mathrm{d}T$ for $YBa_2Cu_3O_{7-x}$ was estimated from the data of $\mathrm{d}v/\mathrm{d}T$ for $BaTiO_3$, where v is the velocity of sound travelling through the sample [14]

$$\mathrm{d}G/\mathrm{d}T = \mathrm{d}E/\mathrm{d}T = 4 \times 10^7 \mathrm{MPa}\,°\mathrm{C}^{-1} \quad (8)$$

The shear modulus at room temperature was estimated using the data of $B = 108$ GPa for the bulk modulus of a single crystal at $x = 0.55$ [15] and 0.28 for the Poisson's ratio, ν, of single-crystal $YBa_2Cu_3O_{7-x}$ [16]. Thus

$$G_{298} = B \times 3(1 - 2\nu)/[2(1 + \nu)]$$
$$= 55.7\ \mathrm{GPa} \quad (9)$$

Combining the above information, we obtain the equation for the shear modulus (in GPa) as a function of temperature (in K)

$$G = G_{298} - (\mathrm{d}G/\mathrm{d}T)(T - 298)$$
$$= 55.7 - 0.04(T - 298) \quad (10)$$

At 850 and 950 °C, G was calculated to be 22.7 and 18.7 GPa, respectively.

3.4. Self diffusivity

Chen *et al.* [10] studied the lattice self-diffusivity of cations in $YBa_2Cu_3O_{7-x}$, and determined the activation energies of yttrium and barium to be 1000 and 890 ± 80 kJ, mol^{-1}, respectively. They also found that the lattice self-diffusion of yttrium is slower than that of barium. It was reported that the lattice self-diffusions of copper and oxygen were much faster than those of yttrium and barium [17–20]. Therefore, yttrium-ion diffusion would control the diffusion of the $YBa_2Cu_3O_{7-x}$ compound and its activation energy for lattice diffusion would be that of the yttrium ion, 1000 kJ mol^{-1}. By the extrapolation of diffusivity data to the zero point of the $1/T$ axis, D_0 was estimated to be $1 \times 10^{25}\ \mathrm{m}^2\,\mathrm{s}^{-1}$.

On the other hand, the grain-boundary diffusivity, D_{gb}, in $YBa_2Cu_3O_{7-x}$ had not been studied, and needed to be estimated. The value of activation energy, 745 kJ mol^{-1}, was taken from the data of superplastic deformation in $YBa_2Cu_3O_{7-x}$ [21, 22]. The frequency factors for grain-boundary diffusion in ceramics, such as MgO, NiO, and ZrO_2, were found within two orders of magnitude to those for the lattice diffusion [23]. Assuming that the frequency factor for the grain-boundary diffusion is the same as that for the lattice diffusion, the diffusivities are estimated as

$$D_l = 1 \times 10^{25} \exp(-1000\,000/RT)\ \mathrm{m}^2\,\mathrm{s}^{-1} \quad (11)$$

$$D_{gb} = 1 \times 10^{25} \exp(-745\,000/RT)\ \mathrm{m}^2\,\mathrm{s}^{-1} \quad (12)$$

where $R = 8.3144$ J mol^{-1}, and T is in Kelvin.

At temperatures of 850 and 950 °C, the diffusivities are $D_l = 3.1 \times 10^{-22}\ \mathrm{m}^2\,\mathrm{s}^{-1}$ and $D_{gb} = 2.2 \times 10^{-10}\ \mathrm{m}^2\,\mathrm{s}^{-1}$ at 850 °C and $D_l = 2.0 \times 10^{-18}\ \mathrm{m}^2\,\mathrm{s}^{-1}$ and $D_{gb} = 1.5 \times 10^{-7}\ \mathrm{m}^2\,\mathrm{s}^{-1}$ at 950 °C.

The unusually large difference between D_l and D_{gb} results, in part, from the very high activation energy for the lattice diffusion (1000 kJ mol^{-1}). A smaller difference between D_l and D_{gb} may be obtained by more flexible assumptions, such as a smaller value of D_0 for grain-boundary diffusion by two orders of magnitude. However, the variation of the estimated value of D_{gb} was found not to affect the map to any great extent, as will be discussed in Section 4.

3.5. Stress exponent and the constant A in the rate equation for power-law creep

There is limited information available on power-law creep (PLC) of $YBa_2Cu_3O_{7-x}$ in the literature. Bussod *et al.* [7] obtained the stress exponent of 2.5 on high-temperature compression tests of $YBa_2Cu_3O_{7-x}$ with a confining pressure of 1 GPa. It was not clear whether the result was originally from the PLC, because there was no supporting information on microstructures. However, the applied stress seems to be sufficiently high, and the result may suggest that the creep rate is proportional to the $(\sigma/G)^3$. Moreover, the stress exponent, n, of 3 seems to be a reasonable assumption according to the general rule for ceramics, i.e. $n \cong 5$ is associated with the presence of five independent slip systems, whereas $n \cong 3$ is associated with either a lack

TABLE II Physical constants used for constructing the deformation mechanism map of $YBa_2Cu_3O_{7-x}$

Symbol	Constant	Value	Unit
Ω	Atomic volume	1.754×10^{-28}	m^3
b	Burgers vector	3.87×10^{-10}	m
δ	Grain-boundary thickness	7.74×10^{-10}	m
G	Shear modulus at 850° C	22.7	GPa
D_l	Lattice diffusivity	$1 \times 10^{25} \exp(-1000000/RT)$	$m^2 s^{-1}$
D_{gb}	Grain-boundary diffusivity	$1 \times 10^{25} \exp(-745000/RT)$	$m^2 s^{-1}$
n	Stress exponent for PLC	3	–
A	Constant for PLC	3	–
B	Constant for NHC	40	–

of five independent slip systems or, if five independent systems are available, a lack of interpenetration of these systems [24]. It is well known that $YBa_2Cu_3O_{7-x}$ has a very limited number of slip systems due to its low-symmetry crystallographic structure. Therefore, a stress exponent of 3 is assumed for the power-law creep in $YBa_2Cu_3O_{7-x}$.

The constant A in the rate equation (Equation 3) was taken to be 3 from the data of MgO and Al_2O_3 [12]. This value is in good agreement with $A = 1$ estimated by the general equation, $n = 3.0 + 0.3 \log A$, with n equal to 3 in the present case. The general equation was established by Stocker and Ashby [25] when they observed a correlation between n and A from a large number of creep data for metals, alloys, ionic and covalent solids, and metal carbides.

All the values for physical constants determined above, as required for constructing the map, are listed in Table II. By substituting the constants in Equations 4–6 with these values, the deformation mechanism map for creep in $YBa_2Cu_3O_{7-x}$ was constructed for temperatures, 850 and 950 °C, as shown in Figs 1 and 2.

4. Discussion

The deformation map constructed shows that at 850 °C the transition from Coble creep to Nabarro–Herring creep occurs at $d/\mathbf{b} \cong 10^{12}$ or $d \cong 10^3$ m. At 950 °C, the transition occurs at a smaller grain size, but its value is still very large, $d \cong 10^2$ m. The predominant role of Coble creep is rather surprising because the lattice diffusion occurs preferably at high temperatures. The reason why the transition occurs at such a large grain size is due to the very high activation energy and the low diffusivity for lattice diffusion. The activation energy for the lattice diffusion in $YBa_2Cu_3O_{7-x}$ is 1000 kJ mol^{-1} [10]. It is much greater than those in perovskite-type compounds, 200–400 kJ mol^{-1} [4], or those of pure metals, which are in the range of 100–200 kJ mol^{-1} [26]. If the ratio of activation energy for grain-boundary diffusion to that for lattice diffusion is 0.6 [12] or 0.75 [21,22], the difference in these activation energies is fairly large, 250–400 kJ mol^{-1}. Thus, the critical grain size for the boundary between NHC and CC becomes very large by the exponential term, $\exp(Q_l - Q_{gb})$, in Equation 4.

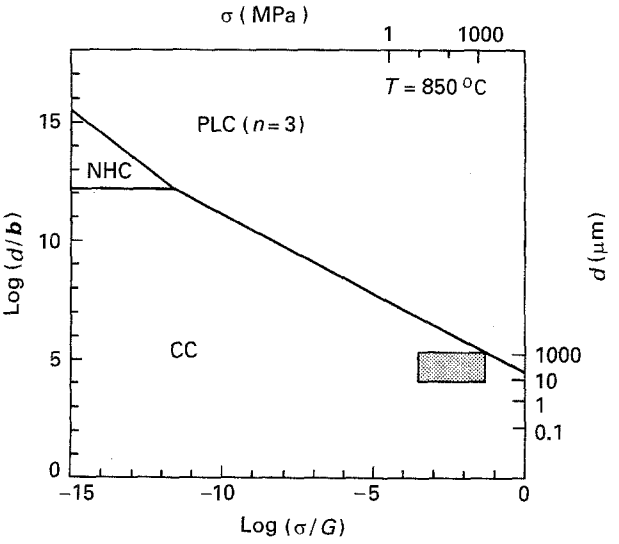

Figure 1 A Langdon-type deformation map for the creep deformation of $YBa_2Cu_3O_{7-x}$ at 850 °C. The shaded rectangle covers the creep data of $YBa_2Cu_3O_{7-x}$.

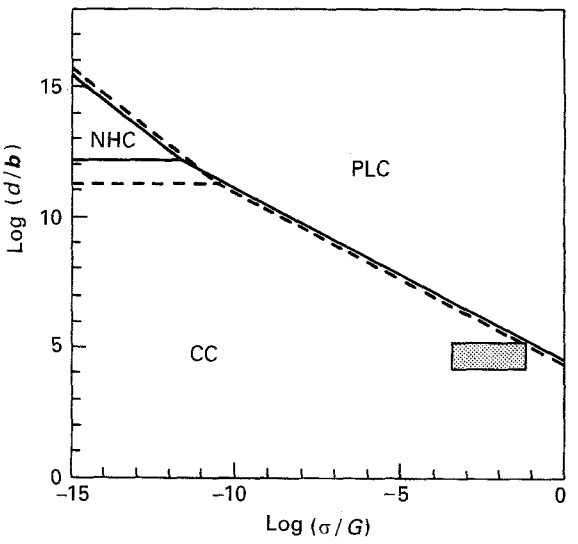

Figure 2 A Langdon-type deformation map for the creep deformation of $YBa_2Cu_3O_{7-x}$ at 950 °C. The shaded rectangle covers the creep data of $YBa_2Cu_3O_{7-x}$. (——) 850 °C, (----) 950 °C.

The constructed map shows that the experimental conditions in the previous studies are inside the domain of Coble creep. This is contradictory to the conclusions made in the earlier studies, which were

interpreted in terms of Nabarro–Herring creep. It should be noticed, however, that these conclusions were not consistent with their experimental observations, such as the grain-size exponent and the activation energy. The grain-size exponent determined by Goretta *et al.* [5] was 2.8, greater than 2 for the Nabarro–Herring creep but close to 3 for the Coble creep. The activation energies determined in the previous studies are generally lower (500–900 kJ mol^{-1}) than that for lattice self diffusion, 1000 kJ mol^{-1}, in $YBa_2Cu_3O_{7-x}$.

As shown in Table I, the activation energies reported for creep are largely scattered from 200–1200 kJ mol^{-1}. However, a careful re-analysis of the data shows that the values may range between 500 and 900 kJ mol^{-1}. Stumberg *et al.* [4] determined the activation energy to be 800 kJ mol^{-1}, which is within the above range. Goretta *et al.* [5] obtained 970 ± 130 kJ mol^{-1} in the temperature range 850–980 °C. However, the data points at 920 °C or above deviated from the straight line, and if these points are ignored, the activation energy is decreased to 680 ± 160 kJ mol^{-1}. Bussod *et al.* [7] reported an unusually low activation energy of 201 kJ mol^{-1}. Their data points were taken at three temperatures, and the data were not linear. Because of the high level of the measured stress (150–950 MPa), their data at the lowest temperature (750 °C) may correspond to a different deformation mechanism, probably the power-law creep, as indicated by the deformation map. If the data points at 750 °C are deleted, the activation energy would be about 800 kJ mol^{-1}. Reyes-Morel *et al.* [6] obtained two activation energies: 565 kJ mol^{-1} at $T < 860$ °C, and 1220 kJ mol^{-1} at $T > 860$ °C. Their data are not on the perfectly straight line, and when curve fitting is practiced in several different slopes, the activation energy would be in the range of 560–760 kJ mol^{-1} at low temperatures. Kodama and Wakai [8] obtained an activation energy of 1080 kJ mol^{-1}. This value is not significant because their samples showed a yield drop due to crack formation in the early stages of testing. It may represent the activation energy for a different process.

When the range of experimental variables, σ and d, from the previous studies, are placed in the map, a rectangle is formed and located very close to the boundary between the domains of Coble creep and power-law creep. Under the condition that the rectangle intersects the boundary ($\sigma \cong 1$ GPa and $d \cong 100$ μm), the rate-controlling mechanism would change from the Coble creep to power-law creep. Indeed, the stress exponent of 2.5, which is close to 3 for the power-law creep, was observed by Bussod *et al.* under similar experimental conditions, i.e. $\sigma = 1$ GPa and $d = 100$ μm. Moreover, a large number of dislocations were observed in the sample tested under similar experimental variables, $d = 50$ μm, $\sigma = 1$ GPa, and $T = 800$ °C [27].

Because the grain-boundary diffusivity, D_{gb}, was estimated by the assumptions, $Q = 745$ kJ mol^{-1} and $D_0 = 1 \times 10^{25}$, D_{gb} may not represent the true value. However, when different values of diffusivity were used to construct the map, the domain of Coble creep would still cover the rectangle, even though the location of the boundary had changed. Fig. 3 shows the change in the location of triple point between HNC, CC, and PLC with the change in the activation energy of grain-boundary diffusion from 500–1000 kJ mol^{-1}. The modified maps clearly show that unless the activation energy for grain-boundary diffusion is abnormally large and close to that of lattice diffusion, the deformation mechanism would be the Coble creep. In a similar way, the predominating role of the Coble creep was also insensitive to the variation of D_0 by plus or minus two orders of magnitude as shown in Fig. 4.

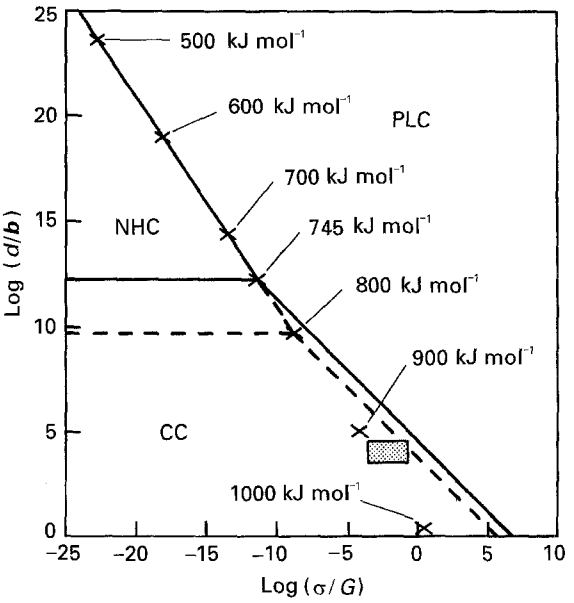

Figure 3 The variation of locations of triple point between domains of the Nabarro–Herring, Coble, and power-law creep as a result of change in assumed values of activation energy for the grain-boundary diffusion from 500–1000 kJ mol^{-1}. The shaded rectangle covers the creep data of $YBa_2Cu_3O_{7-x}$.

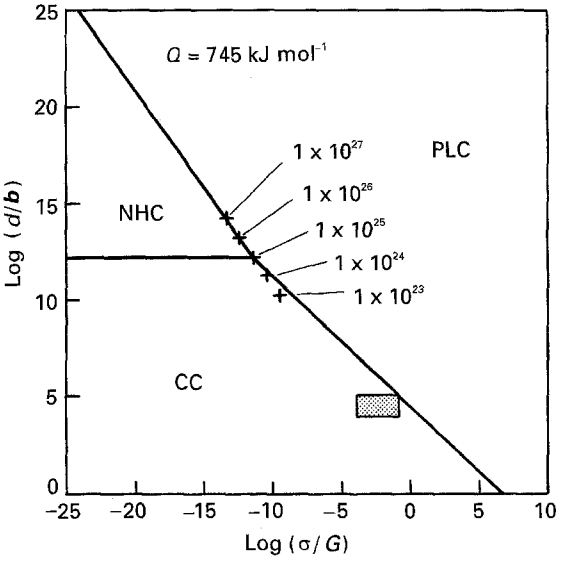

Figure 4 The variation of locations of triple point between domains of the Nabarro–Herring, Coble, and power-law creep as a result of change in assumed values of frequency factors, D_0, by plus or minus two orders of magnitude. The shaded rectangle covers the creep data of $YBa_2Cu_3O_{7-x}$.

5. Conclusions

A Langdon-type deformation mechanism map for creep was constructed and was in reasonable agreement with the experimental results of previous studies. It indicates that even at high temperatures, the Nabarro–Herring creep was unlikely to occur, but instead the Coble creep would predominate in the deformation of the coarse-grained $YBa_2Cu_3O_{7-x}$. It also shows that when the applied stress was as high as 1 GPa, there was a transition from the Coble creep to the power-law creep, which was consistent with the observed intensive dislocation activity and high stress exponent, 2.5. By the use of the deformation map, the discrepancies in the reported data could be explained as the result of a change in the deformation mechanism.

Acknowledgements

The authors gratefully acknowledge helpful discussions with Professors T. G. Langdon and M. R. Notis. They also thank Mr J. M. Albuquerque for his able assistance. The work was supported by the Division of Materials Sciences, United States Department of Energy, under Contract DE-AC05-840R21400 with the Martin Marietta Energy System, Inc.

References

1. M. F. ASHBY, *Acta Metall.* **20** (1972) 887.
2. F. A. MOHAMED and T. G. LANGDON, *Metall. Trans.* **5** (1974) 2339.
3. M. R. NOTIS, in "Deformation of Ceramic Materials", edited by R. C. Bradt and R. E. Tressler (Plenum, New York, 1975) p. 1.
4. A. W. STUMBERG, N. CHEN, K. C. GORETTA and J. L. ROUTBORT, *J. Appl. Phys.* **66** (1989) 2079.
5. K. C. GORETTA, J. L. ROUTBORT, A. C. BIONDO, Y. GAO, A. R. ARELLANO-LOPEZ and A. DOMINGUEZ-RODRIGUEZ, *J. Mater. Res.* **5** (1990) 2766.
6. P. E. REYES-MOREL, X. WU and I.-W. CHEN, in "Ceramic Superconductors II", edited by M. F. Yan (American Ceramic Society, Westerville, Oh, 1988) p. 590.
7. G. BUSSOD, A. PECHENIK, C. CHU and B. DUNN, *J. Am. Ceram. Soc.* **72** (1989) 137.
8. Y. KODAMA and F. WAKAI, in "Advances in Superconductivity II", edited by T. Ishiguro and K. Kajimura (Springer, Tokyo, 1989) p. 113.
9. J. C. BOROFKA, B. C. HENDRIX, A. I. ATTARWALA and J. K. TIEN, *J. Am. Ceram. Soc.* **76** (1993) 1011.
10. N. CHEN, S. J. ROTHMAN and J. L. ROUTBORT, *J. Mater. Res.* **7** (1992) 2308.
11. S. NAKAHARA, S. JIN, R. C. SHERWOOD and T. H. TIEFEL, *Appl. Phys. Lett.* **54** (1989) 1926.
12. T. G. LANGDON and F. A. MOHAMED, *J. Mater. Sci.* **11** (1976) 317.
13. J. JIANG, H. YIN, X. WANG, Y. SUN, F. ZENG and J. DU, *Mater. Sci. Eng.* **B7** (1990) 227.
14. G. MADER, H. MEIXNER and P. KLEINSCHMIDT, *J. Appl. Phys.* **58** (1985) 702.
15. I. V. ALEKSANDROV, A. F. GONCHAROV and S. M. STISHOV, *JETP Lett.* **47** (1988) 428.
16. H. LEDBETTER and M. LEI, *J. Mater. Res.* **6** (1991) 2253.
17. D. GUPTA, S. L. SHINDE, and R. B. LAIBOWITZ, in "High Temperature Superconducting Compounds II", edited by S.H. Whang, A. DasGupta, and R. B. Laibowitz (Minerals, Metals and Materials Society, Warrendale, Pa, 1990) p. 377.
18. J. L. ROUTBORT, S. J. ROTHMAN, N. CHEN, J. N. MUNDY and J. E. BAKER, *Phys. Rev. B.* **43** (1991) 5489.
19. K. N. TU, N. C. YEH, S. I. PARK and C. C. TSUEI, *ibid.* **39** (1989) 304.
20. J. L. TALLON and M. P. STAINES, *J. Appl. Phys.* **68** (1990) 3998.
21. J. YUN, M. P. HARMER and Y. T. CHOU, *Script. Metall. Mater.* **29** (1993) 267.
22. J. YUN, Ph.D. dissertation, Lehigh University, Bethlehm, PA (1994).
23. I. KAUR and W. GUST, in "Handbook of Grain and Interphase Boundary Diffusion Data", Vols 1 and 2 (Ziegler Press, Stuttgart, 1989).
24. A. H. CHOKSHI and T. G. LANGDON, *Mater. Sci. Technol.* **7** (1991) 577.
25. R. L. STOCKER and M. F. ASHBY, *Script. Metall.* **7** (1973) 115.
26. P. G. SHEWMON, "Diffusion in Solids" (McGraw-Hill, New York, 1963) Chs. 6–2.
27. M. J. KRAMER, L. S. CHUMBLEY and R. W. McCALLUM, *J. Mater. Sci.* **25** (1990) 1978.

Received 1 August 1994
and accepted 3 February 1995